Superconducting proximity effect through high-quality high-conductance tunnel barriers

L. Capogna
Dipartimento di Fisica, Università di Salerno, 84081 Baronissi, Salerno, Italy

M. G. Blamire
Department of Materials Science, University of Cambridge, Pembroke Street, Cambridge CB2 3QZ, United Kingdom

(Received 25 September 1995)

The temperature dependence of the critical current of very high-conductance Nb-AlO_x-Al-AlO_x-Nb tunnel junctions with thin middle Al layers (thickness d_{Al} 2–8 nm) shows a tail above the Al critical temperature, whose amplitude strongly depends on d_{Al}. This is interpreted as evidence of a proximity effect through tunnel barriers whose high quality and transparency can be independently assessed. These data have been modeled within the framework of the McMillan model using independently measurable barrier transmission factors, and obtaining an excellent quantitative agreement.

I. INTRODUCTION

Since the pioneering work by Holm and Meissner, many manifestations of the superconducting proximity effect have been reported,[1–3] either between a superconductor (S) and a normal material (N) or between dissimilar superconductors (S,S'). At its simplest, the proximity effect in a bilayer can be viewed as a consequence of a coupling between the two materials which is limited by differences in electronic structure and/or by a physical barrier at the interface. The most complete model of the proximity effect has been obtained within the Usadel formalism by Golubov *et al.*[4] This model has achieved considerable success in reproducing the proximity effect in metal-metal systems, while the earlier Kuprianov-Lukichev theory[5] and the McMillan tunneling model[6] (MTM) have been widely used in the modeling of superconductor-semiconductor[7] and metal-metal[8,9] systems, respectively. Golubov *et al.* have additionally shown that in the limiting case of a low-electron transmission coefficient between the two materials, the relatively simple MTM is derivable from within the more general Usadel formalism for the proximity effect.[4]

However, whichever model has been chosen to represent the proximity effect, the crucial transmission coefficient of the interface between the two proximitized layers has not successfully been measured independently of the proximity effect which it controls.[4] Hence a rigorous quantitative test of the models against experimental data has not been carried out in the systems studied to date (SS',SN,$SINIS$,SSm), even when the interfaces (such as Nb-Cu and Nb-Al) were deposited under ideal conditions in a UHV environment.[4] The transmission coefficient depends entirely and in an unknown way on the properties of the particular bilayer under investigation. Most of the investigated systems[10,11] consist of SN bilayers with various degrees of decoupling between the layers, where it is not possible to derive the transmission coefficient but through the proximity effect. In these systems the MTM has been successfully applied to analyze experiments relating to the critical temperature, to the gaps and tunneling spectra in the gap region in the proximitized bilayer SN. Gilabert *et al.* have also measured[8] the temperature dependence of the critical current in Nb-I-N-Pb junctions with different normal metal N thickness and shown that the observed behavior is well described by numerical calculations of I_c based on the MTM.

There exists a single class of devices in which a fully quantitative test of MTM is possible, i.e., when the proximity effect occurs via an intentionally created tunnel barrier in which the transmission coefficient is directly measurable from the high bias conductance and the quality of the barrier can be assessed by measuring the subgap leakage. However, the technical difficulty of fabricating good quality devices of high conductance and with S' layers thin enough to produce the effect has until now prohibited this type of experiment. Double junction devices $SIS'(N)IS$ were realized in the past[12] to study the proximity effect under the condition of weak SN coupling and a proximitization of the middle layer was detected by studying the dependence of the conductance structures associated to the gaps upon the middle film thickness. However no attention was paid to high-voltage (higher than the sum of the gaps) conductance and the transmission coefficient stayed a free parameter in the fitting procedure to the MTM. In addition, since the barriers were very thick, no Cooper pair tunneling was observed.

An attempt to make an independent estimate of the proximity parameter was carried out by van Huffelen *et al.*[7] in $SSmS$ junctions (Nb-Si-Nb). It was shown that this system behaves like a $SINIS$ structure; in this case the Kupriyanov-Lukichev theory was adopted to describe the temperature dependence of the critical current and the Octavio-Blonder-Tinkham-Klapwijk model was used to figure out the theoretical value for the proximity parameter. However, a large discrepancy was observed between the fitting and the theoretical coupling, probably due to some inhomogeneity in the interface barrier.

In this paper we report, we believe for the first time, a measurable proximity effect through high-conductance $SIS'IS$ tunnel structures, where S' is the proximitized superconductor with equilibrium critical temperature $T_c(S') \ll T_c(S)$. We have used the system Nb-Al-AlO_x-Al-AlO_x-Al-Nb, in which the middle Al layer (Al_{mid}) is proximitized through the AlO_x tunnel barriers by the external Nb-Al proximity electrodes. The high transparency of the

0163-1829/96/53(9)/5683(5)/$10.00 © 1996 The American Physical Society

barriers allows Cooper pairs to tunnel and a critical current has been observed. Analyzing the data in the framework of the MTM has enabled us to fit the temperature dependence of the critical current and then to derive from the fitting procedure the coupling parameter Ψ ($\Psi_{\rm fit}$), defined below, between the proximitized films. Most importantly, an independent value of Ψ ($\Psi_{\rm thy}$) has been derived using the transmission coefficient extracted from the normal-state resistance. We show that an excellent agreement exists between $\Psi_{\rm thy}$ and $\Psi_{\rm fit}$, establishing the quantitative accuracy of both the MTM and the low transmission limit of the Golubov model; we also unambiguously demonstrate a proximity effect through good quality tunnel barriers.

II. DEVICE FABRICATION

The structures we used in this experiment were deposited in sequence without breaking the vacuum in a dual target UHV sputtering system described elsewhere.[13] R-plane sapphire substrates were placed on a substrate holder whose axis of rotation was centered between the Nb and Al targets. During the deposition of all the layers except $\mathrm{Al}_{\rm mid}$ the samples were rotated at constant speed so that repeated passes under the source built up the complete layer. For $\mathrm{Al}_{\rm mid}$, the rotation speed was varied during each rotation so that, with constant source power, a different mean deposition rate applied to each sample. The structures were deposited at ambient temperature with the following thicknesses: $\mathrm{Nb}_{\rm base}$ 100 nm, $\mathrm{Al}_{\rm base}$ 10 nm, AlO_x, $\mathrm{Al}_{\rm mid}$ 2–8 nm, AlO_x, $\mathrm{Al}_{\rm top}$ 5 nm, $\mathrm{Nb}_{\rm top}$ 70 nm. The oxide tunnel barriers were each formed by admitting 10 Pa of pure O_2 for 6 min into the deposition system, followed by a pump-down period of 2 h to ensure full removal of the oxygen. Devices were fabricated using a standard SNEP (Ref. 10) processing route with an anodization stage which permitted the direct measurement of the total Al thickness for each device ($\mathrm{Al}_{\rm base}$ + $\mathrm{Al}_{\rm mid}$ + $\mathrm{Al}_{\rm top}$). We evaluated the $\mathrm{Al}_{\rm mid}$ thickness from the deposition parameters and consequently it is uncorrected for the amount consumed in the oxidation process. We fabricated double junction devices of total specific resistance (R_nA) of order 5×10^{-11} $\Omega\,\mathrm{m}^2$ and current densities as high as 15 kA cm^{-2}. The devices were measured using an Oxford Instruments Heliox ^{3}He insert in the range 0.3–10 K.

III. CURRENT vs VOLTAGE

In Fig. 1 we show typical I-V curves for a device measured at two different temperatures. As expected, the devices show a strong gap enhancement in the $\mathrm{Al}_{\rm mid}$ layer due to nonequilibrium effects;[14] the clear signature of these effects is the step observable at the voltage $2(\Delta_{\rm (Nb\text{-}Al)}-\Delta_{\rm Al_{mid}})/e$ ($\sim$2 mV). However, a nonequilibrium gap in the middle Al electrode can only exist in the limited voltage range between $2(\Delta_{\rm (Nb\text{-}Al)}-\Delta_{\rm Al_{mid}})/e$ and $2(\Delta_{\rm (Nb\text{-}Al)}+\Delta_{\rm Al_{mid}})/e$ (Ref. 15) and an enhancement of $\Delta_{\rm Al_{mid}}$ at zero voltage (as measured by the magnitude of the critical current) cannot be attributed to a nonequilibrium effect of this type. The interpretation of the gap step ($\sim$2.5 mV) is still a subject of debate. If the device was an equilibrium $SIS'IS$ structure below the equilibrium T_c of the Al, then this feature would occur at

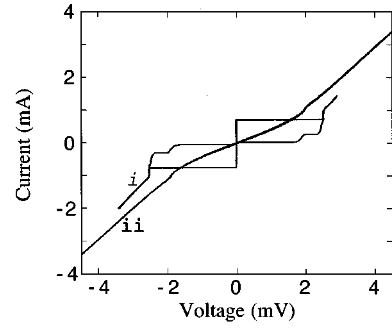

FIG. 1. A typical current voltage curve of 66 $\mu\mathrm{m}^2$ Nb-Al-AlO_x-Al-AlO_x-Al-Nb device with middle Al ($\mathrm{Al}_{\rm mid}$) thickness of 4 nm. Curve (i) $T=1.6$ K, curve (ii) $T=5.8$ K. In (i) the step in the subgap region at the voltage $V_S=2(\Delta_{\rm (Nb\text{-}Al)}-\Delta_{\rm Al_{mid}})\sim2$ meV is the signature of $\mathrm{Al}_{\rm mid}$ gap enhancement due to nonequilibrium effects. The position and the amplitude of this step are strongly temperature dependent.

$2(\Delta_{\rm (Nb\text{-}Al)}+\Delta_{\rm Al_{mid}})/e$ where the gaps would have their equilibrium values. In the nonequilibrium case there is still uncertainty whether there is sufficient extraction of quasiparticles at this bias to maintain the gap in the Al layer above the equilibrium value. According to recent calculations[15] the feature occurs somewhere in between. Later on one will assume that the higher voltage step corresponds to the gap in the external electrodes only. This assumption is justified by the observed temperature dependence of $\Delta_{\rm (Nb\text{-}Al)}$ (Fig. 2). We measure this quantity from the voltages at which the nonequilibrium step and the gap step occur. The nonequilibrium step appears at $V_S=2(\Delta_{\rm (Nb\text{-}Al)}-\Delta_{\rm Al_{mid}})$. As to the gap step, there are two simple assumptions one can make; if one allows the feature at the sum gap to occur at $V_G=2(\Delta_{\rm (Nb\text{-}Al)}+\Delta_{\rm Al_{mid}})$ the derived temperature dependence of $\Delta_{\rm (Nb\text{-}Al)}=(V_G+V_S)/4$ does not follow the BCS temperature dependence (Fig. 2 inset).

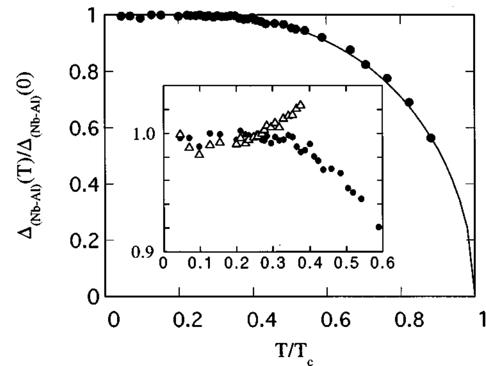

FIG. 2. Temperature dependence (solid circles) of the external electrode gap ($\Delta_{\rm (Nb\text{-}Al)}$) derived from the gap step voltage on the assumption that this corresponds to $V_G=2\Delta_{\rm (Nb\text{-}Al)}$ and no middle Al contribution is present at this bias. The line shows the BCS prediction for comparison. The temperature is normalized to the value $T_c=8.5$ K for the critical temperature in the external electrode. In the inset we compare the data reported in the main figure (solid circles) with the electrode gap derived on the assumption that the gap step occurs at $V'_G=2(\Delta_{\rm (Nb\text{-}Al)}+\Delta_{\rm Al_{mid}})$, that is $\Delta_{\rm (Nb\text{-}Al)}=(V'_G+V_S)/4$ (open triangles).

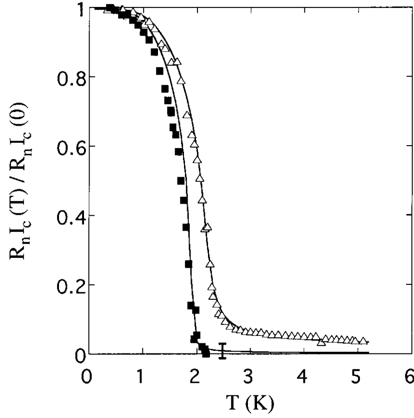

FIG. 3. Temperature dependence of $R_nI_c(T)/R_nI_c(0)$ for two Al_{mid} thicknesses (d_{Al}). Experimental points: triangles, $d_{Al}=2.2$ nm; squares, $d_{Al}=5.6$ nm. The solid lines represent the theoretical MTM fits. An experimental tail does exist in sample with $d_{Al}=5.6$ nm but it is so small as to be in the order of the error.

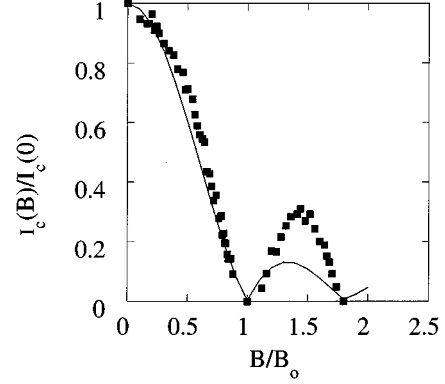

FIG. 4. Magnetic field dependence of $I_c(B)/I_c(0)$ at 4.2 K in a device with $d_{Al}=2.2$ nm. The field is normalized to its value B_0 at the first minimum of $I_c(B)$. The solid line is the theoretical prediction (Ref. 18) for a circular junction $J(x)/x$, where $J(x)$ is the Bessel function of first kind and $x=\pi B/B_0$.

On the contrary, if one supposes that the Al_{mid} does not contribute its gap to the voltage at the gap step, i.e., $V'_G=2\Delta_{(\text{Nb-Al})}$, the temperature dependence of $\Delta_{(\text{Nb-Al})}=V_G/2$ fits very well to the BCS theoretical prediction.

From the *I-V* curves it is evident that the dominant contribution to the current comes from the tunneling processes and that minimal leakage occurs through the AlO_x barriers. The position of the subgap step ($\sim$2 mV) and the magnitude of the observed gap voltage ($\sim$2.5 mV) clearly demonstrate that both junctions are effective, with the gaps in the external proximity Nb-Al electrodes (1.25 meV) being identical to the value reported in single junctions.[16] The normal resistance and the low subgap current both indicate that the two barriers are of similar qualities; no increase in subgap current is observed for bias voltages in excess of $(\Delta_{(\text{Nb-Al})}+\Delta_{\text{Al}_{\text{mid}}})/e$. The quality factor of the devices, V_m ($=I_cR_s$ where R_s is the subgap resistance measured at 1.7 mV and I_c the critical current) is 29 mV, and the ratio R_s/R_n of the subgap resistance to the normal resistance of the whole device is 17.6. Our double-junction structures are of considerably higher quality than the Nb-AlO_x-Nb single junctions fabricated by Miller *et al.*[17] These authors, while investigating the quality of high current density junctions, reported a R_s/R_n ratio of 5 and 10 for devices with $J_c\sim 17$ and 10 kA/cm^2, respectively. To eliminate nonequilibrium effects, the normal resistance R_n of whole device was measured at high voltage bias.

IV. EXPERIMENTAL RESULTS

In our experiments we measured the critical current at zero voltage (the lower critical current of the two observed in the devices) as a function of the temperature $I_c(T)$ in structures with d_{Al} varying in the range 2–8 nm. In Fig. 3 we show typical plots of the ratio $R_nI_c(T)/R_nI_c(0)$ for devices with different d_{Al}. The tail above the critical temperature is the clear signature of the proximity effect, and this is *not observed* in devices with thicker Al_{mid} layers or less transparent barriers. The extension and amplitude of this tail are clearly dependent on d_{Al}; in the devices with the thinnest Al_{mid} layer the tail extends up to 5.2 K. To demonstrate that our devices are well-behaved Josephson tunnel junctions and that the supercurrent in the tail above T_c is a true tunneling current, we investigated the magnetic field dependence of I_c. Figure 4 shows $I_c(B)/I_c(0)$ measured at 4.2 K for a thin Al_{mid} device. The Fraunhofer-type diffraction pattern with full suppression at the minima implies that the conduction occurs uniformly across the barriers and is not dominated by pinholes. It should be noted that the finite floor observed by Miller *et al.*[17] in the minima and by them attributed to the inhomogeneous nature of the barrier, is absent in our pattern, confirming the high quality of the tunnel barriers.

V. COMPARISON OF EXPERIMENTAL OBSERVATIONS AND THEORY

In order to fit the MTM to the $R_nI_c(T)$ data we used the Ambegaoker and Baratoff[19] derivation of $R_nI_c(T)$:

$$R_nI_c(T)=\Delta_{S'}(T)\mathbf{K}\{[1-\Delta^2_{S'}(T)/\Delta^2_S(T)]^{1/2}\},\qquad(1)$$

where $\Delta_{S'}$ is the lower-energy gap and $\mathbf{K}$ is the complete elliptic integral of the first kind. Here we assume that $\Delta_{S'}$ is the energy gap in Al_{mid} induced as a consequence of the proximity effect. We derive $\Delta_{S'}$ from MTM and assume that the layer S' of our devices plays the role of the layer N in MTM. In this model[6] N ($=S'$) and S are assumed to be thin, compared to their respective coherence lengths, and to be weakly coupled by electron tunneling through an interfacial barrier (i.e., small barrier transmission probability); thus the experimental situation fulfills these conditions exactly. These assumptions eliminate the possibility of a spatial dependence of the pair potential. In addition, the transmission probability of electrons incident on the S-S' interface from both sides is assumed to be independent of their energy and direction. Finally it is assumed that the electron-electron interaction is BCS-like and that the films are reasonably clean so that the mean free path is roughly equal to the film thickness. In the model, each film acts as perturbation on the electrons of the other, so that the density of states in each is modified. The important parameters of the theory are $\Gamma_{S'}$ and Γ_S, which are defined as $h/(2\pi\tau_{S'})$ and $h/(2\pi\tau_S)$, respectively, where h is Planck's constant and $\tau_{S(S')}$ is the mean time that an

TABLE I. Data for sample devices. Values for middle Al critical temperature T_c(Al) are obtained: (a) from the maximum value of $dI_c(T)/dT$; (b) as the value giving the best McMillan model (MTM) fits to $R_nI_c(T)$; (c) from the BCS relation $2\Delta_{\rm Al}^{\rm max}=3.5kT_c$, with $\Delta_{\rm Al}$ measured from the positions of the subgap step and of the gap at the lowest possible temperature ($\sim$0.35 K). The experimental $R_nI_c(0)$ product in a double-junction device $[R_nI_c(0)^{\rm ex}]$ is compared with the Ambegaokar and Baratoff prediction $[R_nI_c(0)^{\rm thy}]$ where the lower gap parameter is given by the experimental $\Delta_{\rm Al}(0)$ measured from the IV curves. The factor m is the ratio of $R_nI_c(0)^{\rm ex}$ to the theoretical prediction derived within the MTM. The inverse coupling parameter $\Psi_{\rm fit}=2/(\Gamma_{S'}R_nA)$ is obtained from the measured normal resistance area product R_nA and from the coupling parameter $\Gamma_{S'}$ giving the best MTM fits to $R_nI_c(T)$. In $\Psi_{\rm theor}=2/(\Gamma_{S'}R_nA)$, $\Gamma_{S'}$ is calculated from the transmission coefficient derived from R_nA measurements.

$d_{\rm Al}/2$ (nm)	T_c(Al) (a) (K)	T_c(Al) (b) (K)	T_c(Al) (c) (K)	$I_c(0)R_n^{\rm ex}$ (mV)	$I_c(0)R_n^{\rm thy}$ (mV)	m	$\Psi_{\rm fit}$ $({\rm eV}\,\Omega\,{\rm m}^2)^{-1}$	$\Psi_{\rm thy}$ $({\rm eV}\,\Omega\,{\rm m}^2)^{-1}$
1.1	2.19±0.05	2.15	2.2±0.1	0.96	2.04	0.45	0.022×10^{15}	0.258×10^{15}
1.5	2.31±0.01	2.30	2.4±0.1	1.27	2.17	0.58	0.045×10^{15}	0.349×10^{15}
2.0	2.30±0.01	2.30	2.3±0.1	1.53	2.13	0.69	0.161×10^{15}	0.443×10^{15}
2.8	1.98±0.01	1.90	1.8±0.1	1.50	1.75	0.77	0.345×10^{15}	0.628×10^{15}
3.6	1.79±0.01	1.80	1.6±0.1	1.04	1.63	0.56	0.639×10^{15}	0.812×10^{15}

electron spends in the $S(S')$ layer before tunneling into the other. The Γ_S describe the coupling interaction between S' and S and can be written as follows:

$$\Gamma_{S'(S)}=hv_FD^*8\pi Bd_{S'(S)}, \tag{2}$$

where D^* is the transmission probability of the interfacial tunnel barrier between S' and S, v_F is the Fermi velocity in $S(S')$, $d_{S'(S)}$ is the $(S)S'$ thickness, and B is a function of $d_{S'(S)}$ and the mean free path $I_{S'(S)}$, of order unity. Since MTM considers a single interface, we take $d_{S'}$ to equal $d_{\rm Al}/2$ in our double-junction structure to allow for proximitization through both electrodes.

For a thick S layer MTM gives the expression for the energy gap in S':

$$\Delta_{S'}(T)\cong\frac{\Delta_{S'}^0(T)+\Gamma_{S'}}{1+\Gamma_{S'}/\Delta_S^0(T)}. \tag{3}$$

The fitting procedure, through (1) with $\Delta_{S'}$ given by (3), allowed the determination in each sample of the MTM adjustable parameter $\Gamma_{S'}$ and of the $\rm Al_{mid}$ critical temperature T_c (Table I). As expected the equilibrium critical temperature T_c of $\rm Al_{mid}$ layer was inversely dependent on $d_{\rm Al}$ and never exceeded 2.4 K. The table shows that the best-fit values of T_c are in good agreement with T_c predicted by the BCS expression $2\Delta_{\rm Al_{mid}}=3.5$ K T_c where $\Delta_{\rm Al_{mid}}$ is measured at the lowest temperature ($\sim$0.3 K) from the positions of the nonequilibrium step at $V_s=2(\Delta_{\rm (Nb\text{-}Al)}-\Delta_{\rm Al_{mid}})$ and of the gap step supposed to occur at $V_G=2\Delta_{\rm (Nb\text{-}Al)}$ (Table I). Moreover the fitting T_c agrees for each device with the temperature at which the experimental $|dI_c/dT|$ is maximum, which is the expected value in nonproximitized structures (Table I). These agreements give considerable confidence in the correctness of the fit. In fitting the experimental data, the theoretical value of $R_nI_c(T)$ given by (1) was multiplied by a normalization factor m (Table I) to compensate for the partial suppression of experimental $I_c(T)$ by trapped flux.

In Fig. 2 we show the fitted theoretical $R_nI_c(T)/R_nI_c(0)$ curves for two extreme $d_{\rm Al}$. In all cases the fit is very good, deteriorating only slightly as $d_{\rm Al}$ increases and the strict validity of the assumption that the gap is spatially independent in the Al layer declines. Since the coupling parameter $\Gamma_{S'}$ (2) contains a dependence on the resistance-area product through D^*, we define an inverse coupling parameter Ψ independent of the resistance-area product as follows:

$$\Psi=2/R_nA\Gamma_{S'}, \tag{4}$$

where A is the junction area and the factor of 2 is included in order to get the resistance of a single junction from the whole device R_n. By means of Ψ we have been able to compare devices of different conductance emphasizing only the dependence on the $\rm Al_{mid}$ thickness. In Table I we report the values of $\Psi_{\rm fit}$ calculated from $\Gamma_{S'}$ which fit the data for different $d_{S'}$. In Fig. 5 we plot $\Psi_{\rm fit}$ against $d_{S'}$ together with a least-squares fit to these data which shows a very strong linear dependence of $\Psi_{\rm fit}$ on $d_{S'}$. As a comparison we also plot $\Psi_{\rm thy}$, obtained by calculating $\Gamma_{S'}$ directly from (2) independently from the fitting procedure. In this derivation the transmission coefficient D^* is given by expression (18) from Blonder *et al.*:[20]

$$D^{*-1}=N(0)e^2v_FAR_n, \tag{5}$$

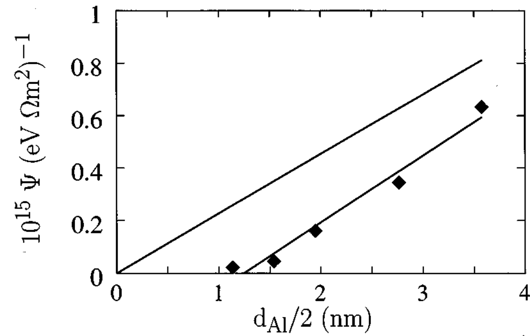

FIG. 5. Dependence of the inverse coupling parameter $\Psi=2/(\Gamma_{S'}R_nA)$ upon $d_{\rm Al}/2$. The points represent $\Psi_{\rm fit}=2/(\Gamma_{S'}R_nA)$ where R_nA is the measured normal resistance area product and $\Gamma_{S'}$ is the coupling parameter giving the best MTM fits to $R_nI_c(T)$. The solid line to the origin is $\Psi_{\rm thy}=2/(\Gamma_{S'}R_nA)$ where $\Gamma_{S'}$ is calculated from the transmission coefficient derived from R_nA measurements. The experimental points are fitted by a linear dependence.

where $N(0)$ is the density of states in the Al_{mid} layer. An excellent agreement is found between the slopes of these two independent derivations of Ψ; the offset in d_{Al} observable in Ψ_{fit} is due to the fact that we are overestimating d_{Al} by ~2 nm. We evaluate d_{Al} from the nominal parameters of deposition; therefore we neglect the reduction of d_{Al} due to its partial oxidation caused by the intentional creation of the upper AlO_x barrier and by the inevitable oxygen diffusion from the lower barrier. However, from our anodization traces we can estimate that the amount of Al consumed in the oxidation process is approximately 1 nm per barrier.

Since the MTM quantitatively describes our data, we can estimate that the order of magnitude of the transmission coefficient of nontunneling channels (from the measured R_s/R_n) is not larger than 10^{-6}. In other words, if we discount the tunneling contribution, we are left with a contribution from leakage effects at least an order of magnitude too small to give the observed proximity effect.

VI. CONCLUSIONS

In our experiment we have detected a clear proximity effect across the good quality barriers of an $SIS'IS$ device. This is an important observation in its own right, given the importance of tunnel-like electron hopping in models of layered high-T_c systems.[21,22] We have demonstrated that our devices are well-behaved Josephson junctions in which the dominant contribution to the current is the tunneling. Most importantly, we have demonstrated that the McMillan tunneling model can be quantitatively applied with no residual adjustable parameters which has not been achieved in any previous work; not only does the model accurately predict the thermal behavior of the critical current, but this fit also gives a value for the coupling parameter which is in excellent quantitative agreement with the value independently extracted from normal resistance measurements.

ACKNOWLEDGMENTS

The authors would like to thank Dr. J. E. Evetts, Dr. R. Monaco, Professor S. Pace, Professor R. D. Parmentier, and Dr. E. J. Tarte for stimulating discussions and careful reading of the manuscript. L.C. was supported by Ministero Universitàe Ricerca Scientifica e Tecnologica (MURST) Italy, and M.G.B. by the Royal Society, UK; this work was partially supported by UK EPSRC and U.S. Naval Research Laboratory, Washington, D.C.

[1] R. Holm and W. Meissner, Z. Phys. **86**, 787 (1933).
[2] J. Clarke, Proc. R. Soc. London, Ser. A **308**, 447 (1969).
[3] J. P. Romagnon, A. Gilabert, J. C. Noiray, and E. Guyon, Solid State Commun. **14**, 83 (1974).
[4] A. A. Golubov, E. P. Houwman, J. G. Gijsberten, V. M. Krasnov, J. Flokstra, H. Rogalla, and M. Yu. Kuprianov, Phys. Rev. B **51**, 1073 (1995).
[5] M. Yu. Kuprianov and V. F. Lukichev, Zh. Éksp. Teor. Fiz. **94**, 139 (1988) [Sov. Phys. JETP **67**, 1163 (1988)].
[6] W. L. McMillan, Phys. Rev. **175**, 537 (1968).
[7] W. M. van Huffelen, T. M. Klapwijck, D. R. Heslinga, M. J. de Boer, and N. van der Post, Phys. Rev. B **47**, 5170 (1993).
[8] A. Gilabert, C. Van Haesendonck, L. Van den Dries, and Y. Bruynserade, Solid State Commun. **31**, 109 (1979).
[9] D. J. Goldie, N. E. Booth, C. Patel, and G. L. Salmon, Phys. Rev. Lett. **64**, 954 (1990).
[10] P. W. Wyatt, R. C. Barker, and A. Yelon, Phys. Rev. B **6**, 4169 (1972).
[11] K. E. Gray, Phys. Rev. Lett. **28**, 959 (1972).
[12] G. I. Lykken and H. H. Soonpa, Phys. Rev. B **8**, 3186 (1973).
[13] M. G. Blamire, R. E. Somekh, Z. Barber, G. W. Morris, and J. E. Evetts, J. Appl. Phys. **64**, 6396 (1988).
[14] M. G. Blamire, E. C. G. Kirk, J. E. Evetts, and T. M. Klapwijk, Phys. Rev. Lett. **66**, 220 (1991).
[15] D. R. Heslinga and T. M. Klapwijk, Phys. Rev. B **47**, 5157 (1993).
[16] P. A. Warburton and M. G. Blamire, IEEE Trans. Appl. Supercond. **3**, 2066 (1993).
[17] R. E. Miller, W. H. Mellison, A. W. Kleinsasser, K. A. Delin, and E. M. Macedo, Appl. Phys. Lett. **63**, 1423 (1993).
[18] A. Barone and G. Paternò, *Physics and Applications of Josephson Effect* (Wiley, New York, 1982).
[19] V. Ambegaoker and A. Baratoff, Phys. Rev. Lett. **10**, 486 (1963).
[20] G. E. Blonder, M. Tinkham, and T. M. Klapwijk, Phys. Rev. B **25**, 4515 (1982).
[21] T. Ito, H. Takagi, S. Ishibashi, T. Ido, and S. Uchido, Nature **350**, 596 (1991).
[22] S. H. Liu and R. A. Klemm, Physica C **216**, 293 (1993).